Journal of Rare Cardiovascular Diseases



RESEARCH ARTICLE

Optimizing β-Sitosterol Nanostructured Lipid Carriers for Enhanced Type II Antidiabetic Effectiveness

Ramsha Aslam¹*, Varsha Tiwari², Prashant Upadhyay³

¹Faculty of Pharmacy, IFTM University, Lodhipur-Rajput, Moradabad, Uttar Pradesh-244102, India

¹Devsthali Vidyapeeth College of Pharmacy, Lalpur, Rudrapur, U.S.Nagar

²Amity Institute of Pharmacy, Amity University, Lucknow, Uttar Pradesh- 226026, India

³School of Pharmaceutical Sciences, IFTM University, Lodhipur-Rajput, Moradabad, Uttar Pradesh-244102, India

*Corresponding Author Ramsha Aslam

Article History

Received: 20.08.2025 Revised: 03.09.2025 Accepted: 18.09.2025 Published: 30.09.2025 Abstract: Introduction: Type II Diabetes Mellitus (T2DM) characterized by Insulin resistance, hyperglycemia, and relative insulin insufficiency is the most common type of DM. The type II diabetes drugs that are now available have several disadvantages, such as high rates of subsequent failure and adverse effects. Herbal treatments have therefore gained increased attention as an alternative approach. Higher plants are abundant in β -Sitosterol (SIT), a lipophilic phytoconstituent that has been shown to have antidiabetic action without causing harmful side effects. We can enhance the solubility and antidiabetic impact of SIT which is poorly soluble by creating a Nanostructured lipid carrier (NLC). Material and method: Melt emulsification followed by ultrasonication technique was used for the preparation of NLC. To create NLC a phytoconstituent SIT was encapsulated in a matrix system formulated by Compritol ATO 888 (solid lipid) and Captex 355 (lipid lipid). We were able to determine the ideal surfactant concentration, solid lipid:liquid lipid ratio, and ultrasonication time that make up an efficient formulation by employing Box-Behnken Design (BBD). A low-dose injection of streptozotocin (40 mg/kg) and a high-fat diet were used to establish type II DM in Wistar rats for four weeks. Studies were conducted on changes in body weight, lipid biomarkers, oral glucose tolerance test (OGTT), and fasting blood glucose (FBG). A pancreatic histological examination was also conducted. Result and Discussion: It was found that the optimized formulation had particle size 79.27 nm, PDI 0.129, and zeta potential -16.4 Mv. Differential scanning calorimetry (DSC) testing revealed that no chemical changes occurred in the optimized formulation. Based on the drug release in-vitro, the NLC continuously released SIT for 28 hours. The fasting blood glucose levels of a high-fat diet (HFD) fed-STZ with SIT-NLC (20 mg/kg) were significantly lower. The levels of TC, TG, and LDL were considerably reduced while the level of HDL was elevated upon oral administration of SIT-NLC (20 mg/kg). Furthermore, the diabetic rats' injured pancreatic tissues were repaired by SIT-NLC. Conclusion: The BBD-generated SIT-loaded NLC was a promising technique for enhancing drug solubility with long-term release. The current investigation reveals that in HFD-STZ-induced diabetic rats, SIT-loaded NLC showed encouraging hypoglycemic activity.

Keywords:

INTRODUCTION

DM is the most prevalent endocrine condition, often developing when there is insufficient or no insulin present, or when insulin function is impaired (insulin resistance)^[1]. Type 1 diabetes and type II diabetes are the two main kinds of DM, with type II accounting for more than 90% of cases^[2]. Insulin insensitivity, hyperglycemia, and hyperinsulinemia are characteristics of type II DM, which is followed by long-term problems. There are a lot of drawbacks to the type II diabetes medications that are currently on the market, including side effects and high rates of secondary failure^[3]. As a result, herbal remedies have drawn more interest as a complementary strategy^[4].

Plant cell membranes naturally contain SIT, a phytosterol that possess a chemical structure with the cholesterol present in mammalian cells. They are widely distributed in plant foods with high lipid content like olive oil, nuts, seeds etc. SIT is a powerful micronutrient that is found in abundance in higher plants and is consumed by mammals through food. ^[5] Numerous scientific studies have confirmed its anxiolytic and sedative properties, as well as its antioxidant, and anti-diabetic activity. SIT has a long history of usage as a medicinal substance with no harmful side effects and is largely acknowledged as a secure and potentially beneficial dietary supplement. ^[6] However, poor water solubility and low oral bioavailability of SIT are among its main disadvantages for clinical application. SIT is an excellent illustration of a lipophilic medication for NLC because of these shortcomings. The development of SIT-loaded NLC may have important clinical ramifications. ^[7] The chemical structure of SIT is shown in Fig.1.



Fig.1: Chemical structure of Beta-Sitosterol

NLC has been introduced as a new and promising drug delivery system. The extremely unordered structures of NLC, boost the capacity for drug loading. NLC remains solid at body and room temperatures. NLC is easily scaled up and produced at a cheap cost. NLC drug delivery systems have various benefits, including good biocompatibility, controlled/sustained drug release, and high bioavailability [8]. The investigation of NLC for drug delivery via several routes, such as oral, pulmonary intravenous injection, nose-to-brain, cutaneous, and ophthalmic applications, has followed. [9].

The purpose of this work was to prepare and optimize SIT-loaded NLC, to make the drug more soluble with sustained and characteristic release, to ensure stable formulation over time, and to improve the antidiabetic potential of SIT.

MATERIAL AND METHODS

2.1 Materials- SIT was procured from Yarrow Chem. Mumbai. Compritol ATO 888, Captex 555, and Phospholipon® 80H from HiMedia, and Tween 80 was purchased from Finar (Ahmedabad). Streptozotocin was procured from Sigma-Aldrich, USA. All the chemicals used were analytical grade, whereas other biochemical kits were obtained from Span Diagnostics Ltd (New Delhi, India). Other analytical grade chemicals used in the study were obtained from the Laboratory of Devsthali Vidyapeeth College of Pharmacy.

2.2 Preparation of SIT-Loaded NLC

The SIT-NLC was prepared by a modified melt emulsification-ultrasonication technique. The solid lipid Compritol 888 (melting point 70 °C), was melted at a temperature 10 °C above its melting point. To obtain a clear solution, Captex 355 (liquid lipid) was then gradually added to the above melted solid lipid. This was done while stirring continuously [10,11]. The aqueous phase, which also contained Phospholipon 80H as a stabilizer and Tween 80 as a surfactant, was heated to the same temperature. To create a pre-emulsion, the aqueous phase was gradually added to the lipid phase while stirring at the same temperature. After that, sonication was applied to this heated pre-emulsion (PCI Analytics Mumbai). Further, a probe sonicator (20:2 on-off cycle) was used to ultrasonicate the heated, homogenous pre-emulsion [12]. To aid in the synthesis of NPs via lipid phase recrystallization, cooling at room temperature was allowed for the preparation of o/w nanoemulsion. Centrifugation of the aqueous NLC dispersion (High-speed Cooling Centrifuge, REMI) eliminated the medication that was not entrapped [13].

2.3 Experimental Design

A randomized response surface BBD was used to optimize the NLC formulation, the effects of the input parameters X1-solid lipid: liquid lipid, X2- surfactant concentration (%), and X3- sonication time (min) on the size (nm) and percent entrapment of NLCs were examined. The independent variables low (-1), medium (0), and high (+1) levels are displayed in Table 1. There were seventeen different combinations produced. The order of these tests was chosen at random.

The experimental design of Box-Behnken developed a non-linear polynomial equation, as given below:

 $Y = b_0 + b_1 X_1 + b_2 X_2 + b_3 X_3 + b_{12} X_1 X_2 + b_{13} X_1 X_3 + b_{23} X_2 X_3 + b_{11} X_1^2 + b_{22} X_2^2 + b_{33} X_3^2$

where Y is the response linked to each factor level combination while b0 is the intercept, b1, b2, and b3 are linear coefficients, b12, b13, and b23 are interaction coefficients, and b11, b22, and b33 are quadratic coefficients generated from the observed values of results from experimental runs.^[14]

Table 1. Independent variables and their coded levels in Box-Behnken design

2 more 24 more persons variables and men coded to vers in Bon Bernmen design							
Independent	Symbol	Coded level					
variable		-1	0	+1			
Drug: solid	X1	1:4:6	1:6:4	1:8:2			
lipid: liquid							
lipid							
Surfactant %	X3	2	3	4			
Sonication	X2	6.0	7.5	9.0			
(min)							



2.4 Characterization

- **2.4.1 Size distribution and polydispersity index:** The Malvern zeta sizer was used to measure the NLC particle size and polydispersity index (PDI). To produce samples with an appropriate scattering intensity, the final NLC suspension was diluted ten times with distilled water. Each value was tested three times at 25 °C ^[14].
- **2.4.2 Entrapment efficiency:** The un-entrapped SIT became separated by dilution with methanol and centrifuged. ^[15,16] After filtering the supernatant, it was measured spectrophotometrically at 209 nm with the same solvent as the blank. According to the following equation, the encapsulation efficiency percentage (EE percent) was determined by the following equation. ^[17]
- % Entrapment efficiency = Total amount of drug- Amount of drug unentrapped X 100

The total amount of drug

- **2.4.3 Zeta potential:** Zeta potential was calculated by Malvern Zetasizer to evaluate the electrophoretic mobility of the optimized SIT-NLC. [18]
- **2.4.4 Shape and surface morphology**: High-resolution imaging from scanning electron microscopy analysis can be used to analyze the surface morphology of optimized SIT-NLC.^[19]
- **2.4.5 DSC:** DSC of the generated NLC to investigate the phase transition characteristics and the effect of thermal variations on the sample's physical condition. DSC (Perkin-Almer) was used to compare the pure drug, pure Compritol ATO 888, and optimized formulation of SIT-NLC in the 30-300 °C scanning range, with a 1-minute holding period at 30 °C. [20]
- **2.4.6** *In-vitro* **release:** Using a dialysis bag technique with a dialysis membrane at 35.5°C, the optimised batch was exposed to in vitro drug release studies for two hours in 0.1N HCl and then for up to twenty-eight hours in phosphate buffer pH 6.8. ^[21] After being carefully weighed out, SIT-loaded NLC dispersions were added to a dialysis bag. The sealed bag was then put in a beaker containing 250 millilitres of physiological solution. ^[22] One millilitre of the receptor phase was extracted and replaced with an equivalent volume of fresh fluid at various time intervals (2, 3, 4, 5, 6, 24, and 28 hours). Every sample was examined by using a UV spectrophotometer.
- **2.4.7 Drug Release Kinetics**: To describe the drug release mechanism, release data were mathematically processed using the zero order, first order, Higuchi diffusion, and Korsmeyer-Peppas models. [23]
- **2.4.8 Stability:** The stability studies were conducted for 90 days at 2–8°C and 25°C/60% RH to assess the drug entrapment and NLC particle size. [24]

2.5 IN-VIVO STUDY

- **2.5.1 Acute Oral Toxicity Study:** An acute toxicity assessment was conducted to investigate any potential toxicity. For SIT-NLC, an acute toxicity investigation was conducted. Four groups with doses of 5 mg/kg, 50 mg/kg, 300 mg/kg, and 2000 mg/kg were used. Animals were fasted 3 hours before dosing. The animals were examined nearly continuously for changes in body weight, mortality, and appearance during the first four hours of their lives, then daily for the next twenty-four hours, and finally every day for the next fourteen days. [25]
- **2.5.2 Induction of T2DM:** For twelve days, male Wistar rats were given time to get acclimated to the lab setting. A normal diet was administered to six rats that were randomly assigned to the normal control group (NC). The other treatment group of animals was then fed with HFD (22% fat, 48%carbohydrate, and 20% protein) for 4 weeks while consuming enough food and water. ^[26]

After a 12-hour fast, the animals were given an intraperitoneal injection of 40 mg/kg of streptozotocin (STZ) diluted in 0.1 M citric acid/sodium citrate buffer, pH 4.5. The raised glucose levels in plasma, which were measured 72 hours after the injection of STZ, indicated hyperglycemia. For the study, rats with fasting blood sugar levels between 180 and 280 mg/dl were chosen.^[27]

2.5.3 Experimental design

At least six wistar rats each were divided into control and preventive groups. All dosing of standard and test samples was done orally throughout the experimentation.

Group I: Normal control, rats received vehicle,

Group II: Diabetic control (DC) (STZ- 40 mg/kg bw),

Group III: Standard medication Metformin (250 mg/kg) was administered to diabetic rats.

Group IV: Rats treated with test samples BS-NLC (20 mg/kg) bw p.o.

Every weekend, all of the rats had a 12-hour fast before having their FBG levels checked. Body weights were measured on 0, 14, 21, and 28 days of the experiment.



- **2.5.4 Oral Glucose Tolerance Test:** Rats that have been given diabetes underwent OGTT. At the end of the twenty-first day, an OGTT was conducted. Blood was collected via retro-orbital plexus after an 8-hour fasting to measure blood glucose levels (0 min). After that, an oral D-glucose solution (2 g/kg body weight) was given to all rats. Every group had blood collected at 30, 60, 90, and 120 minutes, and the plasma glucose level was recorded. [28]
- **2.5.5 Investigation parameters:** The parameters studied were Body weight, Blood glucose level and lipid profile. The serum parameters were studied after sacrificing the animals at study termination.
- **2.5.6 Histopathology:** For histopathological analysis, the pancreatic specimens were dipped in a solution of formalin (10%). These tissues underwent processing, including dehydration in various alcohol grades, clearing in toluene, and impregnation for predetermined lengths of time in molten paraffin wax, which were then left to solidify. To show overall tissue structure, sections were cut, dried, and stained with 1% aqueous eosin and hematoxylin. Stained slides were cleaned with xylene, dehydrated in progressively higher grades of alcohol, and mounted in Canada balsam. The sections were examined under a microscope with $\times 10$ objective lenses. [29]

RESULTS AND OBSERVATIONS:

Based on the 17 experimental runs produced by BBD (Table 2), the preparation of the SIT-loaded NLCs was done using the method described in the literature, with a little modification. All of the observed responses were compared and assessed to select the most appropriate experimental parameter.

3.1.1 Effect of process variables on particle size and entrapment efficiency: The graph displayed an initial decrease in the size of the particle followed by a considerable increase. The change might be the consequence of an early rise in solid lipids, which will offer the perfect mix of liquid and solid lipids, resulting in the smallest size of particles. On the other hand, when the concentration of solid lipids increases, more solid material accumulates therefore particle size increases. Furthermore, a significant drop in particle size was first seen with an increase in surfactant concentration, and then there was a minor increase in particle size with additional surfactant concentration. The first increase in surfactant concentration is intended to promote stability by reducing interfacial tension. After the saturation point is reached for the surfactant concentration, additional increases result in the deposition of surplus molecules of surfactant on the NLC surface, which again causes rise in size. The duration of ultrasonication had no discernible impact on the size of the particles. As the ultrasonication period was increased, only little variations were noticed. Fig. 2 (A-C) gives the effects of multiple independent parameters on particle size.

 $Size = +128.87 + 43.61 \text{ A} - 42.07 \text{ B} + 2.25 \text{ C} + 51.76 \text{ A} \text{B} - 18.28 \text{ A} \text{ C} - 13.44 \text{ B} \text{ C} + 128.52 \text{ A}^2 + 106.34 \text{ B}^2 + 47.85 \text{ C}^2$

The solid/liquid lipid ratio significantly increased the percentage of entrapment efficiency in the 3D response surface plot, followed by a slight fall. This may be because the solubilization of the drug was facilitated by the initial rise in solid lipid concentration. Increases in the lipid ratio further contributed to an excessive decrease in the liquid lipid content, which reduced the drug entrapment level in the NLC matrix's liquid compartment and encouraged the drug expulsion from the solid matrix once it was entrapped. Similar to this, a rise in surfactant concentration and ultrasonication duration first produced an increasing entrapment efficiency curve, which was then followed by a fall with more improvement. A higher concentration of surfactant may improve the solubility of the drug in both the lipid and aqueous phases and aid in its partitioning. The ejection of the drug from the lipid matrix resulted in a decrease in entrapment efficiency, and the lipid matrix may become saturated with more surfactant. However, the use of ultrasonication facilitated entrapment of drug by transferring the drug molecules in the lipid matrix from the aqueous phase; additionally, extending the duration of the sonication may result in the expulsion of the drug that is partially attached to the matrix. Figure 2 (D-F) gives more detailed information on the effects of multiple independent parameters on entrapment efficiency.

Otimised formulation was selected by analysing the effect of independent parameters on dependent responses. Further evaluation parameters were conducted on F1 formulation.

3.1.2 Particle size, PDI, and entrapment efficiency: The optimized SIT-loaded NLC particle size was 79.27 nm, indicating the formation of nanoparticles. Enhanced bioavailability has been demonstrated by nanoparticles because of their smaller size. The extremely low PDI value of 0.129, which indicates a limited size distribution, provides more evidence for the uniform particle distribution. Fig. 3 displays the particle size graph for the optimized formulation.

A significant finding is the entrapment efficiency of 95.69% for optimized SIT-NLC. A high entrapment efficiency indicates that the medication is effectively trapped in a significant amount within the lipid matrix, hence avoiding drug leakage. Drug molecules can more easily become entrapped in a highly disordered structure created by a mixture of liquid and solid lipids. Certain lipids, such as medium-chain triglycerides (Captex 355), produce amorphous solid-state NLC that prevent drug expulsion because they do not crystallize.



Table 2. BBD matrix with predicted and observed response

	X1	X2	X3	X3 Response 1			Response 2		
Formulations	Solid: liquid lipid ratio	Surfactant Concentrat- ion	Ultrasonicat ion time	Size observed	Size Predicted	%EE observed	%EE Predicted		
		%	min	nm	nm	%	%		
F1	0	0	0	79.27	128.87	95.69	93.29		
F2	0	1	1	210.31	229.80	69.36	71.96		
F3	0	0	0	185.33	128.87	95.56	93.29		
F4	-1	-1	0	383.57	413.94	84.46	83.61		
F5	0	-1	-1	309.43	309.43	80.93	78.33		
F6	0	-1	1	341.73	340.82	69.37	71.71		
F7	-1	0	-1	251.89	241.01	74.56	78.01		
F8	0	0	0	96.89	128.87	90.48	93.29		
F9	0	0	0	141.65	128.87	92.86	93.29		
F10	0	1	-1	251.27	252.18	79.61	77.27		
F11	1	0	1	321.84	332.72	82.73	79.28		
F12	-1	0	1	311.72	282.26	77.61	76.12		
F13	1	0	-1	335.51	364.97	87.82	89.31		
F14	1	-1	0	407.61	397.64	81.79	82.90		
F15	-1	1	0	216.32	226.29	76.38	75.27		
F16	0	0	0	141.21	128.87	95.27	93.29		
F17	1	1	0	447.39	417.02	89.58	90.43		

 $Entrapment = +93.29 + 3.61 A - 0.2025 \ B - 2.98 C + 3.97 \ AB - 2.04 AC + 0.3275 \ BC - 2.19 \ A^2 - 8.05 \ B^2 - 10.42 \ C^2$

Size	Entrapment
(A)	(D)

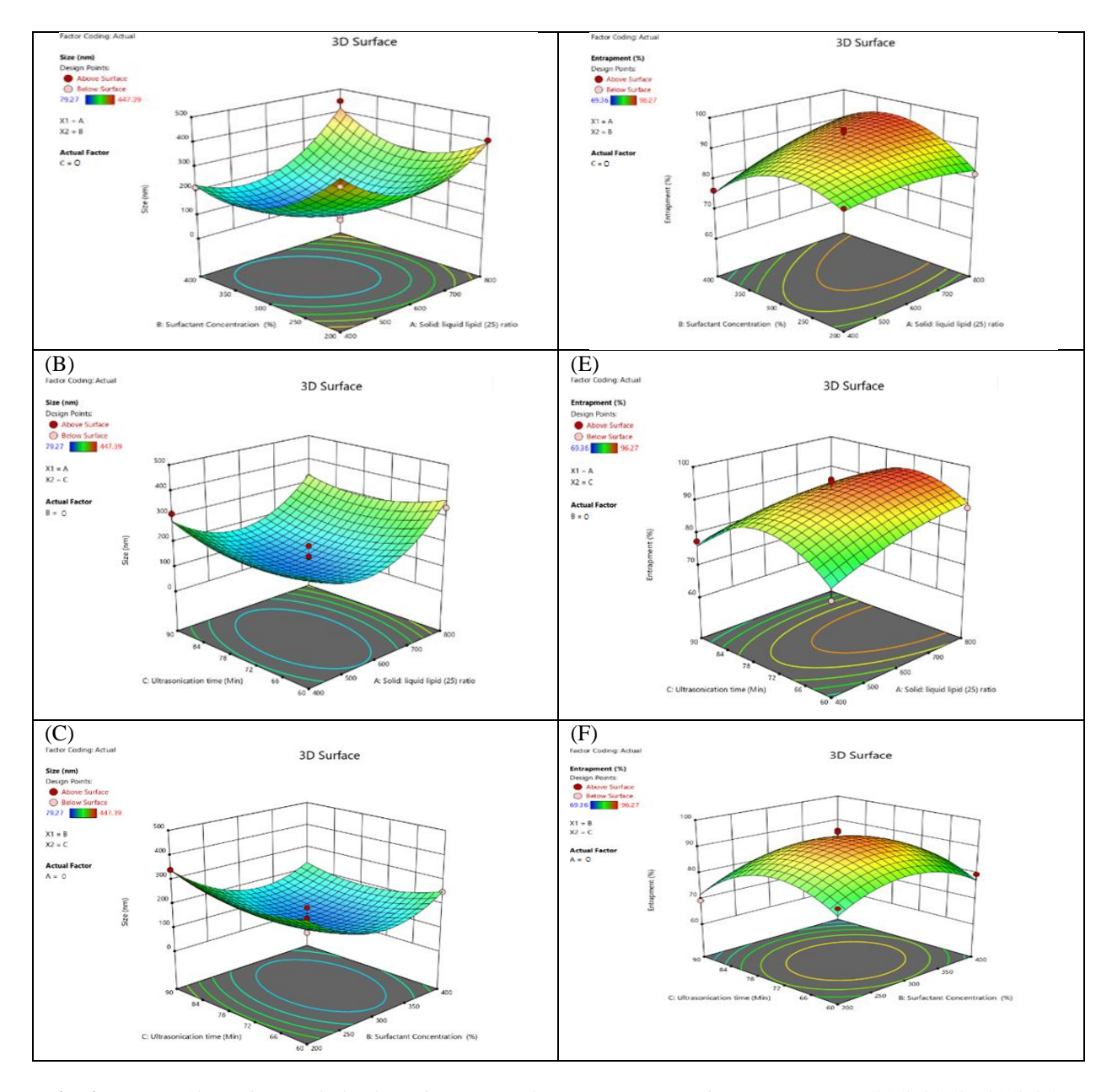


Fig. 2: 3D graphic surface optimization of (A) NLC size (nm) versus surfactant (%) and solid lipid: liquid lipid (B) NLC size (nm) versus sonication time (min) and solid lipid: liquid lipid (C) NLC size (nm) versus sonication time (min) and surfactant (%), (D) %EE versus surfactant (%) and solid lipid: liquid lipid (E) %EE versus sonication time (min) and solid lipid: liquid lipid (F) %EE versus sonication time (min) and surfactant (%)

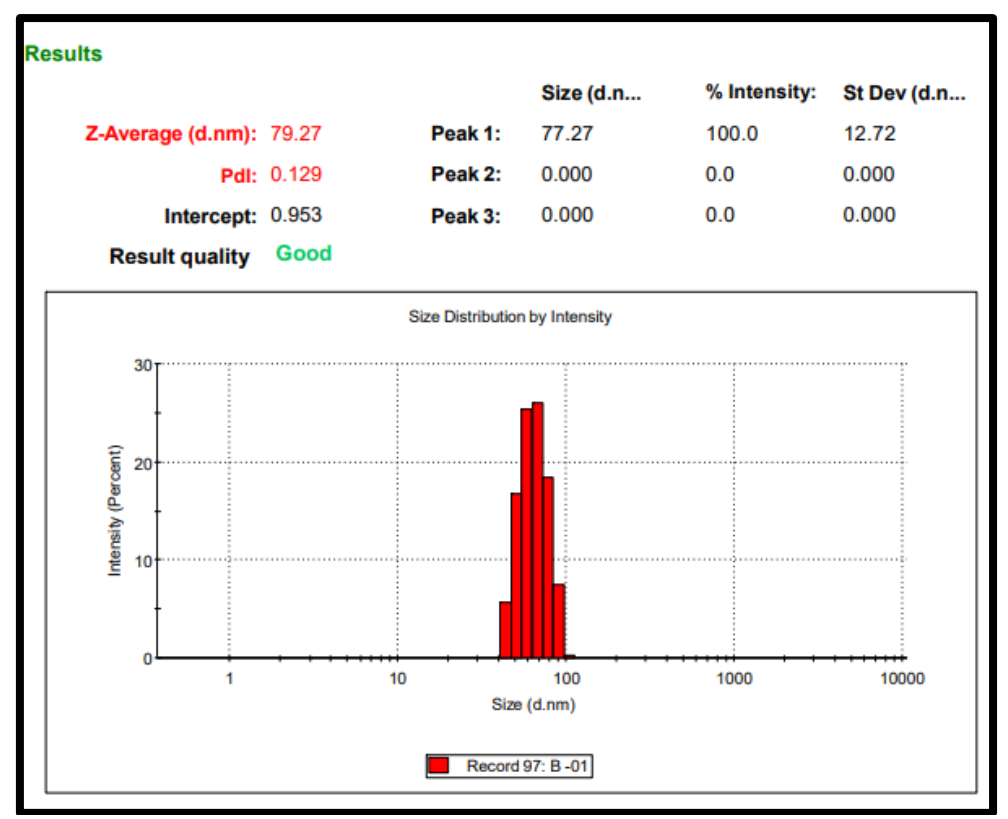


Fig. 3: The particle size graph of the optimized SIT-NLC formulation

3.1.3 Zeta Potential: The stability of colloidal dispersion is influenced by zeta potential. The optimized SIT-NLC formulation was -16.4 mV, showing the colloidal dispersion's long-term stability without aggregation. In the colloidal system, electrostatically stable particles are also recognized by negative zeta potential values. Fig. 4 displays the zeta potential plot for the optimized formulation.

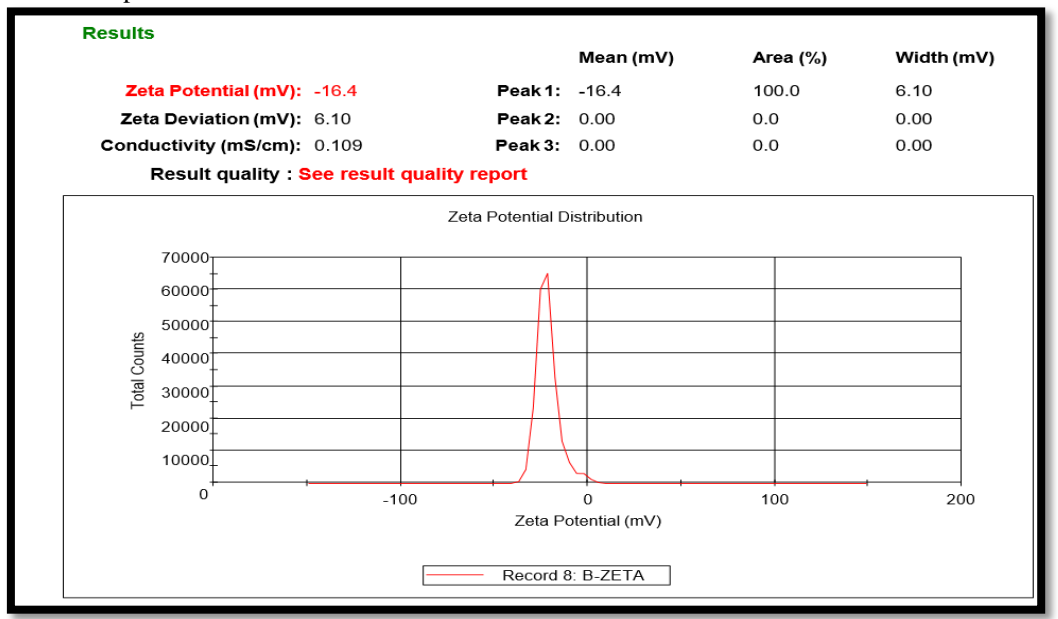


Fig. 4: The Zeta Potential graph of the optimized SIT-NLC formulation

3.1.4 Scanning Electron Microscopy- As seen in Fig. 5, SEM images of SIT-NLC were tiny, uniformly sized, spherical particles at magnifications 8.07KX.

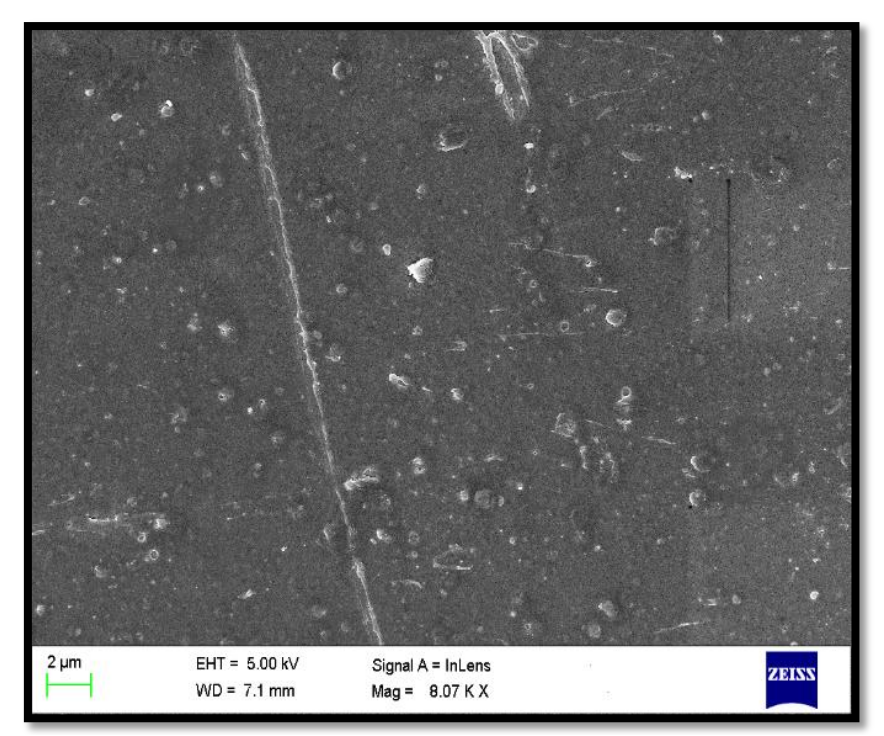
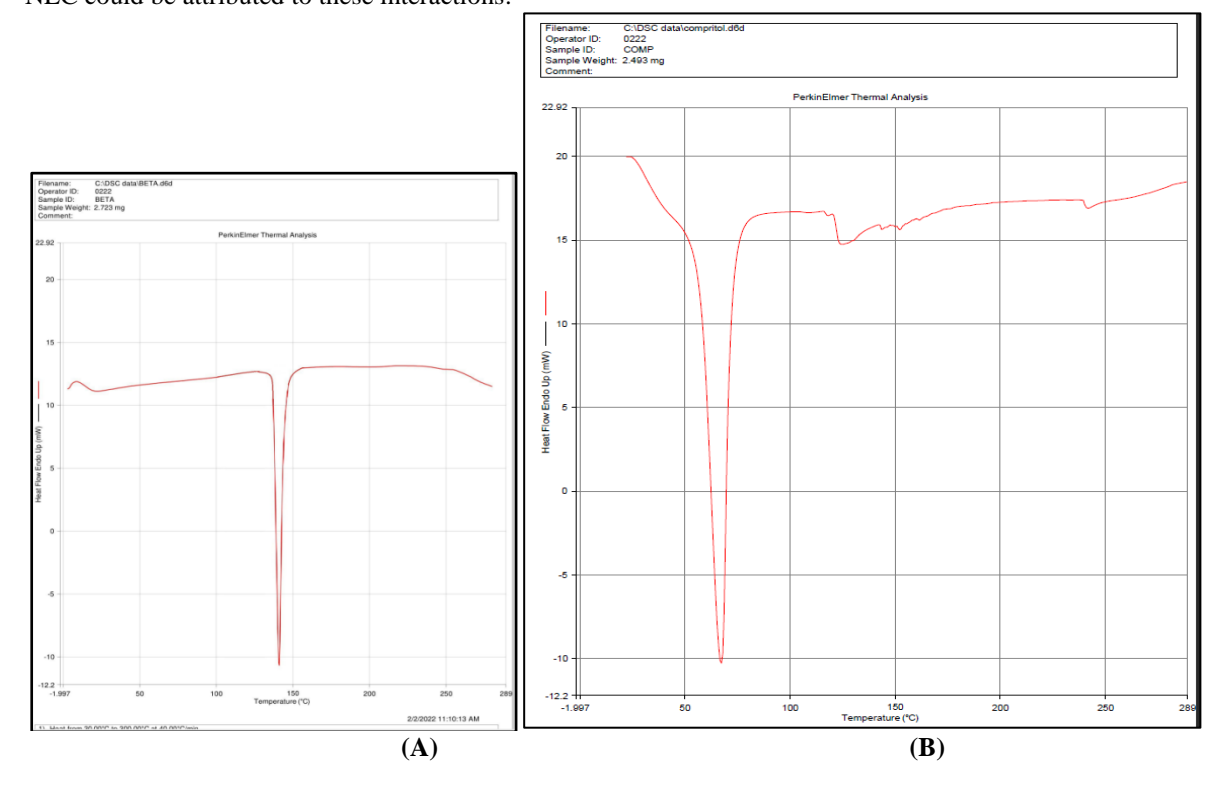


Fig. 5: SEM of the optimized SIT-NLC formulation

3.1.5 Differential scanning colorimetry- The DSC analysis provided insights into the thermal behavior of the components within the formulation. The thermogram of SIT and Compritol ATO 888 showed sharp peaks at 140°C (Fig. 6A) and 72°C (Fig. 6B) respectively. Due to interactions between the drug and other formulation ingredients, the DSC of the optimized formulation (Fig.6C)exhibits broadband. The improved solubility and prolonged release of SIT from the NLC could be attributed to these interactions. [24]



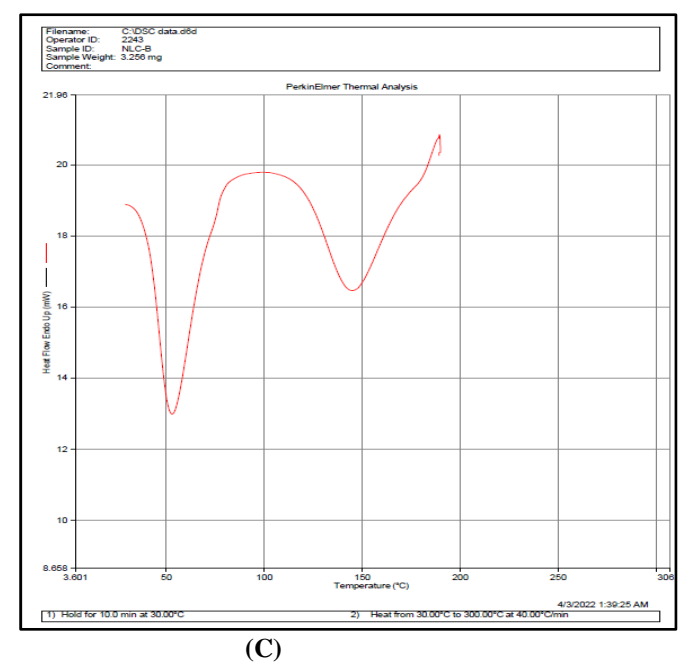


Fig. 6: Thermogram of (A)SIT, (B) Compritol ATO 888 (C) Optimised SIT-NLC formulation

3.1.6 *In-vitro* **release** – The in vitro drug release from solid lipid nanoparticles was studied for up to 28 hours using the dialysis bag technique initially in 0.1N HCl for 2 hours further in phosphate buffer pH 6.8. The results showed that SIT has a hydrophobic nature and only releases 31.24% in 28 hrs. After 28 hours, 78.13% of the drug was released from the optimised formulation. Fig. 7 shows the SIT pure and optimised formulation's in vitro drug release profile.

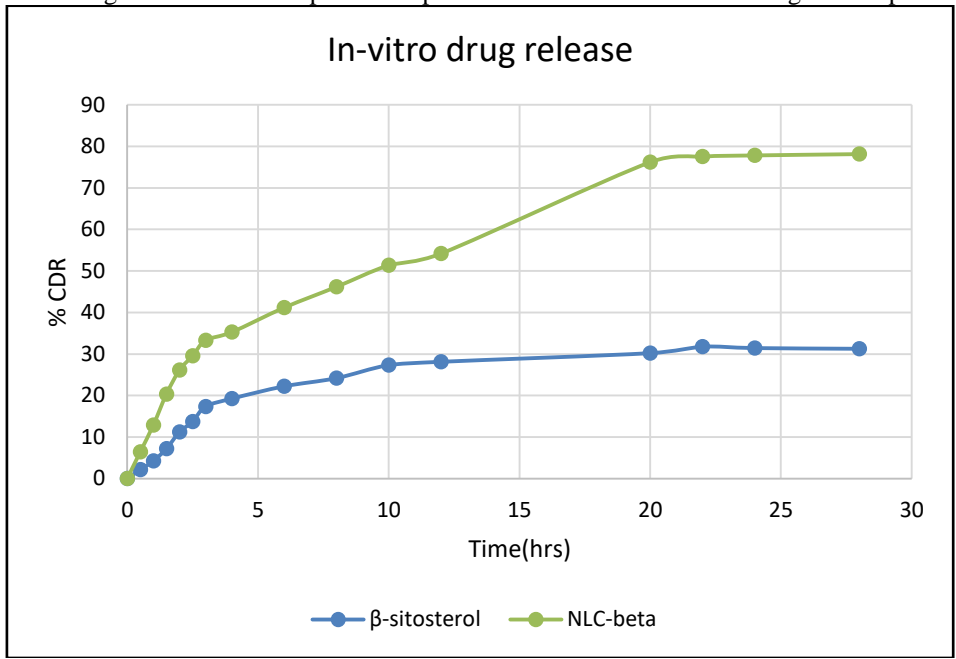


Fig. 7: In-vitro release of pure SIT and optimized SIT-NLC formulation

3.1.7 Drug Release Kinetics- The release data was mathematically analyzed using the Higuchi diffusion, zero order, first order, Korsmeyer-Peppas, Hixson-Crowell, and Higuchi diffusion models to explain the drug release pattern. The regression coefficient R2 value for the Higuchi model is closer to 1, i.e., 0.9829 indicates release by diffusion through a matrix system, as can be seen from the data shown in Fig. 8.

30

6.000

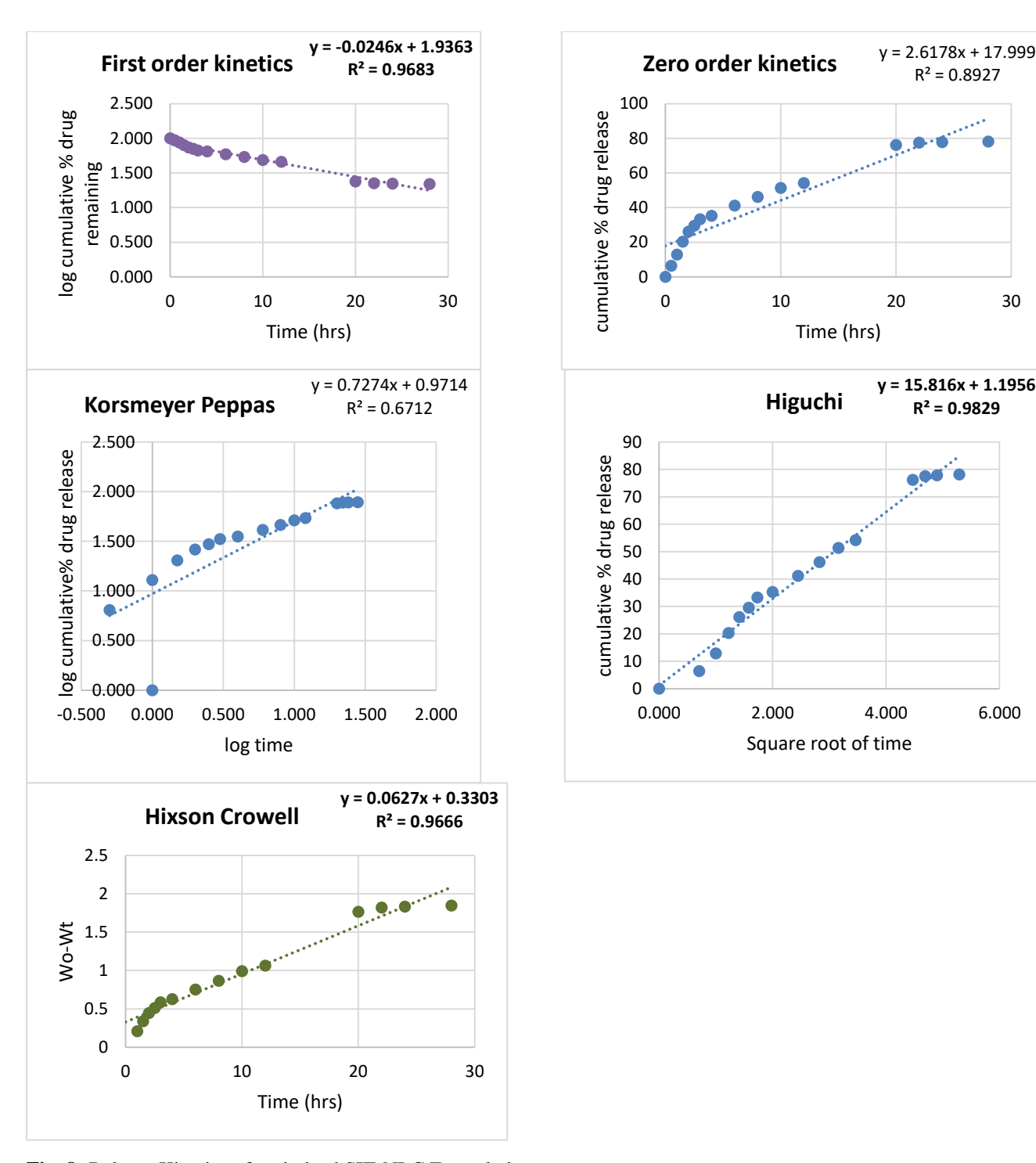


Fig. 8: Release Kinetics of optimized SIT-NLC Formulation

3.1.8 Stability Studies- Particle size and drug entrapment efficiency were the subjects of stability analysis on the optimized formulation that was manufactured and stored under different conditions. The formulation was checked at various periods. Table 3 indicates that no noticeable alteration in the particle size and entrapment effectiveness was noted under either the regular or accelerated temperature and humidity conditions. It is, therefore, possible to conclude that the optimized formulation was suitably stable during the whole period, even if the changes were not sufficiently significant to warrant consideration.



Table 3	3. Sta	bility	studies
---------	---------------	--------	---------

Storage condition		Particle size (nm)			Entrapment Efficiency (%)			
Condition	Initial	30 days	60 days	90 days	Initial	30 days	60 days	90 days
2-8°C	79.27	81.15	85.67	88.39	95.69	95.27	94.61	92.34
25°C/60% RH	79.27	83.38	86.58	90.56	95.69	93.85	90.88	89.16

3.2 IN-VIVO STUDY

Type II diabetes is known to produce hyperlipidemia and hyperglycemia in humans because of insulin resistance in skeletal muscle, liver tissues, and adipose tissue, among other peripheral. A high-fat diet combined with a small dosage of streptozotocin is known to cause the pancreatic β -cells to rapidly degrade, resulting in decreased glucose-stimulated insulin release and insulin resistance. These are two hallmarks of type II diabetes. [3]

PPAR- γ controls the expression of genes related to fat, glucose, and insulin signaling. In type II DM models, PPAR γ is abundantly expressed in white adipose tissue and its increase improves insulin sensitivity. Insulin resistance in rats is brought on by tissue-specific PPAR γ downregulation. In diabetic rats, SIT reduce insulin resistance via upregulating PPAR- γ expression. [32]

Insulin suppresses the synthesis of glucose in the liver and increases the absorption of glucose by GLUT4 in muscle and adipose tissue, which lowers blood glucose levels. Rats fed a high-fat diet and made diabetic by streptozotocin stimulate muscle GLUT4 expression through decreased hexokinase activity, decreased glycogen content, and increased plasma glucose. SIT increases the expression of PPARγ in adipose tissue and GLUT4 in muscle, indicating that SIT is an insulin-sensitizing agent and may be an alternate medication for the treatment of type II diabetes. [33]

3.2.1 Acute toxicity studies - Studies on acute toxicity showed that the test sample SIT-NLC did not significantly alter the behavior of the animals as measured by body weight, urination, food and water intake, respiration, convulsion, tremor, constipation, changes in skin and eye colors, etc.

3.2.2 Effect of SIT-NLC on body weight in HFD fed-STZ induced diabetic rats

The body weight of rats is displayed in Table 4. When compared to diabetic control rats, the four-week treatment of SIT-NLC (20 mg/kg) did not result in a statistically significant alteration in body weight.

Table 4. Variations in body weight in normal control, diabetic control, standard, and Test sample SIT-NLC groups

Group No.	Treatment	Days							
		0	3	7	14	21			
I.	Normal Control	192.23 ±3.019	194.05 ±2.733	197.46 ±3.228	201.63 ±3.794	205.97 ±3.870			
II.	Diabetic Control	199.55 ±3.146	209.24 ±2.674	217.51 ±3.720	228.22 ±3.472	235.65 ±3.621			
III.	Diabetic+ Metformin (250 mg/kg)	201.85 ±3.477	206.59 ±5.056	212.04 ±5.079	215.19 ±4.995	211.72 ±4.841			
IV.	Diabetic+SIT-NLC (20 mg/kg)	203.49 ±3.861	209.35 ±4.750	215.62 ±5.226	218.37 ±5.403	215.64 ±5.661			

3.2.3 Effect of SIT-NLC on FBG in HFD fed-STZ-induced diabetic rats

The levels of FBG in experimental and control rats are displayed in Table 5. The poor glucose tolerance was evident in Group II; in contrast, the blood glucose levels of the diabetic+SIT-NLC group considerably decreased (P < 0.001).

3.2.4 Effect of Test samples SIT-NLC on fasting OGTT level

The blood glucose levels in each group of experimental rats grew progressively after receiving glucose orally for 30 minutes, as seen in Table 6. Compared to diabetic control rats, there was a substantial (P < 0.001) normalization in blood glucose levels in diabetic rats treated with SIT-NLC (20 mg/kg).



Table 5. Variations in BGL after 0, 1, 3, 7, 14 and 21 days of treatment period

Group	Group Treatment Days						
No.		0	3	7	14	21	
I.	Normal Control	91.16±5.879	91.66±4.844	92.66±4.131	93.83±3.869	94.00±3.406	
II.	Diabetic Control	273.00±7.925	285.33±8.914	299.50±11.743	323.33±11.396	329.83±16.339	
III.	Diabetic+ Standard Metformin (250 mg/kg)	292.16±7.305	248.33±4.803	186.00±3.033	144.66±3.445	104.16±3.430	
IV.	Diabetic+SIT-NLC (20 mg/kg)	276.16±10.834	251.00±7.294	209.66±6.802	176.83±9.786	146.66±9.709	

Table 6. Variations in BGL after 0, 30, 60, 90, and 120 min of the treatment period

Group No.	Treatment								
		0 min	30 min	60 min	90 min	120 min			
I.	Normal Control	92.83±1.472	179.16±10.284	144.83±7.521	104.16±3.601	99.166±3.817			
II.	Diabetic Control	310.66±5.820	418.66±6.532	391.00±7.731	362.16±9.160	334.5±9.160			
III.	Diabetic+ Standard Metformin (250 mg/kg)	97.00±4.561	225.00±7.043	165.66±8.937	125.33±3.011	105.00±6.261			
IV.	Diabetic+SIT- NLC (20 mg/kg)	137.66±3.445	248.83±12.287	180.50±16.742	134.33±9.070	117.16±17.589			

3.2.5 Effect of Test samples BS-NLC and DI-NLC on serum lipid profile

Oral administration of SIT-NLC (20 mg/kg) significantly lowered the levels of TC, TG, and LDL and raised the level of HDL, when compared to untreated diabetic rats as given in Table 7. When SIT-NLC was given to diabetic rats, it significantly corrected the alterations in their lipid profile.

Table 7. Variations in lipid profile in normal control, diabetic control, standard, and Test sample SIT-NLC groups

Group	Treatment	TC	TG	HDL	LDL
No.					
I.	Normal Control	101.01±0.615	97.86±1.438	45.65±8.171	34.59±8.346
II.	Diabetic Control	147.15±1.702	164.98±16.145	15.75±1.460	98.41±2.091
III.	Diabetic+ Standard Metformin	108.69±1.323	88.65±1.228	44.44±5.358	37.25±11.433
	(250 mg/kg)				
IV.	Diabetic+SIT-NLC (20 mg/kg)	123.03±1.052	119.19±8.579	32.68±2.679	66.52±3.163

3.2.6 Histopathological analysis: Rat pancreas from group I showing normal islets of Langerhans including β -cells in the center. Group II: Rat pancreas showing partial degeneration, necrosis and vacuolisation of islets of Langerhans. There were intralobular and interlobular ducts seen. Group III: Slides from the group receiving standard medication treatment displaying islet cells dotted throughout the acinar cells. Compared to the acinar cells around them, the islets had a lighter stain. Group IC: Slides from the SIT-NLC treated group demonstrate number of islet cells in comparison to cells in Group II.

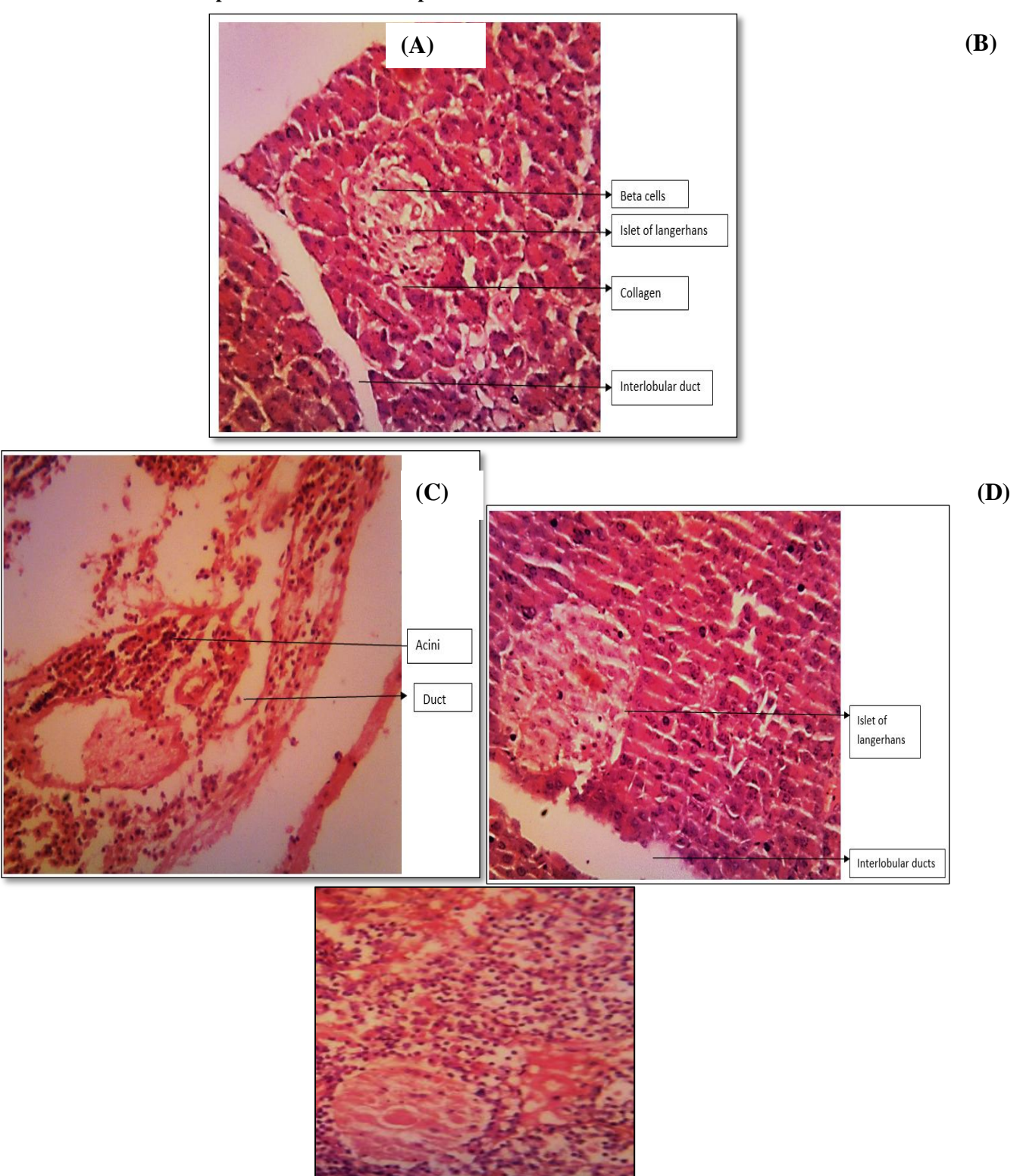


Fig. 8: Histological analysis of (A) Group I (B) Group II (C) Group III (D) Group IV



CONCLUSION

The design and optimization of SIT- NLC for the treatment of Type II DM were presented in the present work. A modified melt emulsification technique combined with ultrasonication was used to effectively create the drug-loaded NLC. Randomized response surface approach, including BBD, was utilised for both experimental design and optimization. The goal was to develop stable, biodegradable, nanostructured lipid carriers with enhanced sustained release and drug entrapment characteristics. The NLC generated by BBD is utilized to produce a potential strategy to improve drugs solubility and long term stability. SIT-NLC demonstrated strong antihyperglycemic, antihyperlipidemic, and pancreatic protective effects in Type II DM rats, according to the results of the in vivo activity. As a result, SIT-NLC may be a useful Type II antidiabetic medication and a potential substitute for type DM.

REFERENCES

- 1. Patel AK, Manigauha A. Antioxidant and antidiabetic activity of isolated flavonoids from Alangium salvifolium leaves extracts. Int J Green Pharm 2018; 12 (2): 82-90.
- Kavitha K, Sujatha1 K, Manoharan S. Development, Characterization and Antidiabetic Potentials of Nilgirianthus ciliatus Nees Derived Nanoparticles, J Nanomed Biother Discov 2017; 7 (2)" 2-11.
- 3. Kharroubi AT, Darwish HM, Diabetes mellitus: The epidemic of the century. World J Diabetes 2015; 6(6): 850–867.
- 4. Aba1 PE, Asuzu IU. Mechanisms of actions of some bioactive anti-diabetic principles from phytochemicals of medicinal plants: A review. Indian J Nat Prod and Resour 2018; 9(2): 85-96.
- Dwivedi J, Sachan P, Wal P. A mechanistic approach on structural, analytical and pharmacological potential of beta-sitosterol: A promi sing nutraceutical. Curr Nutr Food Sci 2024; 20(8): 932-51.
- 6. Lade U, Agrawal S, Barsagade P, Gotefode S, Agrawal T. Formula tion of solid lipid nanoparticles using beta-sitosterol and its characteri zation. Int J Pharm Res Appl 2021; 6(4): 486-91.
- 7. Hu FQ, Jiang SP, Du YZ, Yuan H, Ye YQ, Zeng S. Preparation and characterization of stearic acid nanostructured lipid carriers by solvent diffusion method in an aqueous system. Colloids Surf B Biointerfaces 2005; 45(3-4): 167-73.
- 8. Ghasemiyeh P, Samani SM. Solid lipid nanoparticles and nanostructured lipid carriers as novel drug delivery systems: applications, advantages and disadvantages. Res Pharm Sci 2018; 13(4): 288–303.
- Poovi G, Vijayakumar TM, Damodharan N. Solid Lipid Nanoparticles and Nanostructured Lipid Carriers: A Review of the Effect of

- Physicochemical Formulation Factors in the Optimization Process, Different Preparation Technique, Characterization, and Toxicity. Curr Nanosci 2019; 15(5): 436-453.
- Viegas C, Patrício AB, Prata JM, Nadhman A, Chintamaneni PK, Fonte P. Solid lipid nanoparticles vs. nanostructured lipid carriers: A comparative review. Pharmaceutics 2023; 15(6): 1593.
- 11. Gadhave DG, Kokare CR. Nanostructured lipid carriers engineered for intranasal delivery of teriflunomide in multiple sclerosis: Optimization and in vivo studies. Drug Dev Ind Pharm 2019; 45(5): 839-51.
- 12. Agrawal M, Saraf S, Pradhan M, et al. Design and optimization of curcumin loaded nano lipid carrier system using box-behnken design. Biomed Pharmacother 2021; 141: 111919.
- 13. Bukke SPN, Venkatesh C, Bandenahalli Rajanna S, et al. Solid lipid nanocarriers for drug delivery: Design innovations and characteriza tion strategies—a comprehensive review. Discov App Sci 2024; 6(6): 279.
- 14. Lasoń E, Sikora E, Ogonowski J. Influence of process parameters on properties of nanostructured lipid carriers (NLC) formulation. Acta Biochim Pol 2013; 60(4): 773-7.
- 15. Nandini PT, Doijad RC, Shivakumar HN, Dandagi PM. Formulation and evaluation of gemcitabine-loaded solid lipid nanoparticles. Drug Deliv 2015; 22(5): 647-51.
- Zhuang CY, Li N, Wang M, et al. Preparation and characterization of vinpocetine loaded nanostructured lipid carriers (NLC) for improved oral bioavailability. Int J Pharm 2010; 394(1-2): 179-85.
- 17. Anuradha K, Senthil KM. Development of Lacidipine loaded nano structured lipid carriers (NLCs) for bioavailability enhancement. Int J Pharm Med Res 2014; 2(2): 50-7.
- 18. Koppel DE. Analysis of macromolecular polydispersity in intensity correlation spectroscopy: the method of cumulants. J Chem Phys 1972; 57: 4814-4820.
- 19. Abdelbary G, Fahmy RH. Diazepam-loaded solid lipid nanoparticles: design and characterization. AAPS PharmSciTech 2009; 10(1): 211-9.
- 20. Dudhipala N, Ettireddy S, Youssef AAA, Puchchakayala G. Deve lopment and in vivo pharmacokinetic and pharmacodynamic evaluation of an oral innovative cyclodextrin complexed lipid nanoparticles of irbesartan formulation for enhanced bioavailability. Nanotherano stics 2023; 7(1): 117-27.
- 21. Singh S, Kamal SS, Sharma A, Kaur D, Katual MK, Kumar R. Formulation and in-vitro evaluation of solid lipid nanoparticles containing Levosulpiride. Med Mater Sci 2017; 4(1): 17-29.



- 22. Costa P, Sousa Lobo JM. Modeling and comparison of dissolution profiles. Eur J Pharm Sci 2001; 13(2): 123-33.
- 23. Shetty C, Babubhai S, Pathan I. Development of valdecoxib topical gels–effect of formulation variables on the release of valdecoxib. Int J Pharm Pharm Sci 2010; 2: 70-3.
- 24. Thakkar H, Desai J, Parmar M. Application of boxbehnken design for optimization of formulation parameters for nanostructured lipid car riers of candesartan cilexetil. Asian J Pharm 2014; 8(2): 81.
- Rameshwar GS, Venkatrao PU, Vithalrao NA, Pramodrao AM. OECD Guidelines for Acute Oral Toxicity Studies: An Overview. Int. J. Res. Avurveda Pharm 2023:14:137-40.
- 26. Zhang M, Lv XY, Li J, Xu ZG, Chen L. The characterization of high-fat diet and multiple low-dose streptozotocin induced type 2 diabetes rat model. J Diabetes Res 2008; 2008(1):704045.
- 27. Antony PJ, Gandhi GR, Stalin A, Balakrishna K, Toppo E, Sivasankaran K, Ignacimuthu S, Al-Dhabi NA. Myoinositol ameliorates high-fat diet and streptozotocin-induced diabetes in rats through promoting insulin receptor signaling. Biomed Pharmacother 2017; 88: 1098-113.
- 28. Jiao Y, Wang X, Jiang X, Kong F, Wang S, Yan C. Antidiabetic effects of Morus alba fruit polysaccharides on high-fat diet-and streptozotocin-induced type 2 diabetes in rats. J ethnopharmacol 2017; 199: 119-27.
- Zhuang CY, Li N, Wang M, Zhang XN, Pan WS, Peng JJ, Pan YS, Tang X. Preparation and characterization of vinpocetine loaded nanostructured lipid carriers (NLC) for improved oral bioavailability. Int J Pharm 2010; 394(1-2): 179-185.
- 30. Thapa A, Ahad M, Aqil SS, Imam YS. Formulation and optimization of nanostructured lipid carriers to enhance oral bioavailability of telmisartan using Box–Behnken design. J Drug Deliv Sci Technol 2018; 44: 431–439.
- 31. Qadir A, Aqil M, Ali A, Warsi MH, Mujeeb M, Ahmad FJ, Ahmad S, Beg S. Nanostructured lipidic carriers for dual drug delivery in the management of psoriasis: systematic optimization, dermatokinetic and preclinical evaluation. J. Drug Deliv. Sci. Technol 2020; 57: 101775.
- 32. Jayaraman S, Devarajan N, Rajagopal P, Babu S, Ganesan SK, Veeraraghavan VP, Palanisamy CP, Cui B, Periyasamy V, Chandrasekar K. β-Sitosterol circumvents obesity induced inflammation and insulin resistance by down-regulating IKKβ/NF-κB and JNK signaling pathway in adipocytes of type 2 diabetic rats. Molecules 2021; 26(7): 2101.
- 33. Ramalingam S, Packirisamy M, Karuppiah M, Vasu G, Gopalakrishnan R, Gothandam K, Thiruppathi M. Effect of β-sitosterol on glucose homeostasis by sensitization of insulin resistance via enhanced protein expression of PPRγ and glucose transporter 4 in high fat diet and

streptozotocin-induced diabetic rats. Cytotechnology 2020; 72(3):357-66.